Dispersion compensation in whispering gallery modes

Vladimir S. Ilchenko, Anatoliy A. Savchenkov, Andrey B. Matsko, and Lute Maleki

Jet Propulsion Laboratory, California Institute of Technology,
4800 Oak Grove Drive, Pasadena, California 91109-8099

We show that manipulation by a spatial profile of refractive index of a circularly symmetric dielectric cavity results in a novel way of fine tuning frequency separations as well as spatial localizations of high-Q whispering gallery modes excited in the cavity. The method enables dispersion compensation in the modes (spectrum equalization), diminishes the the quality-factor limitation by surface roughness and contamination, and enables critical coupling to ultra-high-Q modes without maintaining an air-gap with evanescent couplers.

I. INTRODUCTION

Optical cavities consisting of two or more mirrors are utilized in all branches of modern linear and nonlinear optics. Practical usage of such cavities is technically restricted, especially when high performance of the devices, i.e. high quality factor and high mode stability, is important. Fabrication of good optical mirrors, their alinement, and binding are rather expensive and difficult tasks.

Open dielectric microcavities may become an alternative for usual optical cavities. Fabrication of these microcavities is rather simple and inexpensive. The cavities demonstrate high mode stability and high quality factors. High-Q optical microcavities with whispering-gallery modes (WGM) [1–4] are already in the core of many evolving photonics applications such as high-stability narrow linewidth microlasers [5–15], high resolution spectroscopy, remote sensing, and opto-electronic oscillators [16–22], to optical memory devices,true-time optical delay lines, and optical switching devices [23–27].

However, there are significant differences between properties of open dielectric microcavities and conventional optical cavities constructed of mirrors. Originally proposed spherical whispering gallery mode microcavities (microspheres) are over-moded, with complex quasi-periodic spectrum and unequal mode spacings translating from both material and cavity dispersion. Significant reduction in the mode spectral density is achieved in highly oblate spheroidal microcavity (microtorus) [28], but still current fabrication technologies cannot produce dielectric microcavities with equidistant spectra.

Performance and range of applications based on WGM microcavities will be significantly expanded if a method is found to make microcavity modes equally spaced with precision corresponding to a fraction of the resonance bandwidth. Such a dielectric microcavity with equidistant mode spectrum is similar to the Fabry-Perot resonator. A dielectric cavity with equidistant spectrum may be used, for example, in frequency comb generators, optical pulse generators, broad band energy storage circuits of electro-optical devices, and in other applications where conventional optical cavities are utilized.

Within current technology based on uniform resonator material, the smaller is the cavity size, the more the cavity dispersion is manifested in unequal spectral separation between adjacent modes. The problem is rooted in the fact that the radial distribution of whispering gallery resonant modes is frequency dependent. Higher frequency modes propagate on paths that are slightly closer to the surface than those of lower frequency modes. Thus, higher frequency modes travel in trajectories of slightly larger radius, and slightly longer optical path lengths.

Optical path length is a function of both the physical distance and the index of refraction. We propose to fabricate a cavity out of a cylindrically symmetric material whose index decreases in the radial direction. With the proper choice of a gradient of the refractive index circular trajectories corresponding to WGM at different frequencies will have identical optical path lengths. This results in equidistant mode spectrum of the cavity.

We show that mode confinement is also changed in a cavity made from a graded-index material [29]. The position of the maximum of the field of each mode shifts toward the cavity center, mode volumes are increased and displaced away from the surface, thereby desensitizing the quality factor from the effects of surface contamination and roughness. Both these effects are identified currently as the main factor preventing the improvement of Q towards the fundamental limit imposed by bulk material attenuation. Therefore we predict a substantial increase of the mode quality factor in graded index cavities.

Finally, "burying" the mode volume well inside the resonator helps to address the technical problem of maintaining the tunnelling gap between high-Q WGM cavity and evanescent wave coupler device. With appropriate engineering, critical coupling will be obtained under full mechanical contact with the coupler.

II. WHISPERING GALLERY MODES: BASICS

Let us consider a dielectric sphere with dielectric constant distribution $\epsilon(r)$ which depends on the radius r only. The electric field in the sphere obeys to the Maxwell

equation

$$\nabla \times (\nabla \times \mathbf{E}) + \frac{\epsilon(r)}{c^2}\frac{\partial^2 \mathbf{E}}{\partial t^2} = 0, \quad (1)$$

where c is the speed of light in the vacuum. Presenting the electric field as $\mathbf{E} = \int_0^\infty d\omega \mathbf{e}(r)\exp(-i\omega t)$, we rewrite the above equation as

$$\nabla \times (\nabla \times \mathbf{e}) - k^2\epsilon(r)\mathbf{e} = 0, \quad (2)$$

where $k = \omega/c$ is the wave vector. Eq.(2) may be solved in terms of TE and TM modes. Taking in mind that $\nabla \cdot (\epsilon \mathbf{e}) = 0$ we write

$$\mathbf{e} = \sum_{\nu,m} \frac{1}{r}\left[\Psi \mathbf{Y}_{\nu,m} + \frac{1}{\epsilon(r)}\nabla \times (\Phi \mathbf{Y}_{\nu,m})\right], \quad (3)$$

where radial functions Ψ and Φ stand for TE and TM modes respectively, $\mathbf{Y}_{\nu,m}$ are vector spherical functions with angular number ν and magnetic number m. It worth noting that modes of an infinite dielectric cylinder may be described in a similar way.

Radial field distribution for TE modes [30] of a dielectric cavity (sphere or cylinder) can be described by equation

$$\frac{\partial^2 \Psi}{\partial r^2} + \left[k^2\epsilon(r) - \frac{\nu(\nu+1)}{r^2}\right]\Psi = 0, \quad (4)$$

where ν is angular momentum number ($\nu = 0, 1, 2, 3, \ldots$ for a sphere, $\nu = 1/2, 3/2, 5/2, \ldots$ for an infinite cylinder). Electric field distribution has a dependence $\Psi(r)/r$ for a sphere, and $\Psi(r)/\sqrt{r}$ for a cylinder.

Equation (4) has an exact solution for homogeneous dielectric cavity $\epsilon(r) = \epsilon_0 = \text{const}$. This solution reads $\Psi(r) = J_{\nu+1/2}(kr)$, where $J_{\nu+1/2}(kr)$ is the Bessel function of the first kind. The mode spectrum is determined by the boundary conditions $\Psi(r) \to 0$ for $r \to \infty$ and 0, where R is the radius of the sphere or cylinder. In the case of high mode order $\nu \gg 1$

$$k_{\nu,q} \simeq \frac{1}{R\sqrt{\epsilon_0}} \times \left[\nu + \alpha_q\left(\frac{\nu}{2}\right)^{1/3} - \sqrt{\frac{\epsilon_0}{\epsilon_0 - 1}} + \frac{3\alpha_q^2}{20}\left(\frac{2}{\nu}\right)^{1/3} + O\left(\nu^{-2/3}\right)\right] \quad (5)$$

where a_q is the qth root of the Airy function, $Ai(-z)$, which is equal to 2.338, 4.088, and 5.521 for $q = 1, 2, 3$, respectively [31].

The first order approximation for the mode eigenfunctions and eigenvalues may be found from the solution of an approximate equation

$$\frac{\partial^2 \Psi}{\partial r'^2} + \left(k^2\epsilon_0 - \frac{\nu(\nu+1)}{R^2} - r'\frac{2\nu(\nu+1)}{R^3}\right)\Psi = 0, \quad (6)$$

where we assume that $\nu \gg 1$, $r' = R - r$, $\Psi(0) = \Psi(R) = 0$. Comparison of the numerical solution of the exact equation (4) and of the approximate equation (6) shows that the solution of (6) gives satisfactory results for the eigenvalues as well as eigenfunctions of the exact problem.

To describe dispersion of the modes we compare a value equal to the ratio of frequency separations between two pairs of neighboring modes and the mode width. The number of equidistant modes in the case of large ν can be estimated as

$$N = \max_q \left| \left(\frac{\partial^2 k_{\nu,q}}{\partial \nu^2}\right)^{-1} \frac{k_{\nu,q}}{2Q} \right|. \quad (7)$$

From Eq. (5) we derive

$$N_1 \simeq 1.2\,\frac{\nu^{8/3}}{Q}. \quad (8)$$

The mode dispersion can be very high for realistic conditions. For example, for $\nu = 10^3$ cavity modes can already be treated as un-equidistant for $Q \geq 10^8$. Keeping in mind that maximum achieved quality factor for a whispering gallery mode is 9×10^9 [3] one can see that the dispersion problem is in fact quite important.

III. WHISPERING GALLERY MODES IN A CAVITY MADE OF A GRADED DIELECTRIC

A. Dispersion compensation for the main mode sequence

Let us now study the mode spectrum of a dielectric cavity with spatially distributed refractive index

$$\epsilon(r) = \epsilon_0 + \epsilon'(R - r). \quad (9)$$

We show in the following that choosing ratio between constants ϵ_0 and ϵ' in an appropriate way one is able to suppress the mode dispersion significantly.

Exact analytical solutions of Eq.(4) with $\epsilon(r)$ determined by (9) is rather difficult to obtain. We therefore simplify the problem by assuming that the radius of the cavity is large enough $R \gg \lambda$, where λ is optical wavelength in the material. In this case $\nu \gg 1$ and almost all the energy of the mode is confined nearby the surface of the cavity in a layer having a thickness $\sim R\nu^{-2/3}$. Introducing $r' = R - r$ we decompose Eq.(4) assuming that $1 \gg r'/R$

$$\frac{\partial^2 \Psi}{\partial r'^2} + \left[\left(k^2\epsilon_0 - \frac{\nu(\nu+1)}{R^2}\right) - r'\left(\frac{2\nu(\nu+1)}{R^3} - k^2\epsilon'\right)\right]\Psi = 0. \quad (10)$$

This equation has an exact solution

$$\Psi_q(r') = \Psi_{q,0} Ai\left[\left(\frac{2\nu(\nu+1)}{R^3} - k_q^2\epsilon'\right)^{1/3}\frac{r'}{\alpha_q} - \alpha_q\right], \quad (11)$$

where $\Psi_{q,0}$ is the field amplitude, k_q is the root of the equation

$$k_q^2\epsilon_0 - \frac{\nu(\nu+1)}{R^2} = \alpha_q \left(\frac{2\nu(\nu+1)}{R^3} - k_q^2\epsilon'\right)^{2/3}. \quad (12)$$

It is easy to see that Eq.(12) gives a close approximation of the first two terms of the decomposition (5) if $\epsilon' = 0$. For nonzero ϵ' we get

$$k_{\nu,q} \simeq \frac{1}{R\sqrt{\epsilon_0}} \times \left[\nu + \alpha_q \left(\frac{\nu}{2}\right)^{1/3} \left(1 - \frac{R}{2}\frac{\epsilon'}{\epsilon_0}\right)^{2/3}\right] \quad (13)$$

The number of equidistant modes for the cavity can be found from (7) and (13)

$$N_2 \simeq 1.2\,\frac{\nu^{8/3}}{Q}\left(1 - \frac{R}{2}\frac{\epsilon'}{\epsilon_0}\right)^{-2/3}. \quad (14)$$

Therefore, if $\epsilon' \to 2\epsilon_0/R$ the cavity has, to the first order, an equidistant frequency spectrum. Our numerical solution of the exact problem, presented in Fig.1, confirms the results derived from the analytical solution.

B. Dispersion compensation for the radial mode spectrum

Surprisingly, except for ν-dispersion compensation, a graded material cavity demonstrates radial dispersion compensation (index q) Fig.2. This happens because modes do not encounter the cavity boundaries for large refractive index gradients, but only the potential dip created due to the gradient. As a consequence, radial profiles of cavity modes are nearly symmetrical, much in the same way as harmonic oscillator wave functions (see inset of Fig.2).

This conclusion follows from complex angular momentum theory [32]. In this theory an analogy between optics and mechanics is utilized and the cavity modes are described as eigenvalues of an effective potential U. For the whispering gallery modes with index ν this potential may be written as a sum of an attractive wall of depth $(\epsilon(r) - 1)k^2$ with the centrifugal potential $\nu(\nu+1)/r^2$.

The potential is asymmetric when ϵ does not depend on radius r inside the sphere (see Fig.3, solid line). In the spheres possessing dielectric susceptibilities increasing to the sphere center the potential pocket broadens, shifts into the the cavity, and becomes more symmetric. The minimum of the potential is still on the sphere surface. For the critical value of the susceptibility gradient the potential resembles a half of the oscillatory potential $U \sim (r-R)^2|_{r\to R-0}$ (see Fig.3, short dash). For the gradients beyond the critical value the minimum of the potential moves into the cavity. The deeper is the minimum of the potential the better it can be described by the oscillatory potential (Fig.3, long dash).

C. Engineering the cavity field distribution for improving mode quality factors

The gradient in the index of refraction affects the field distribution in the cavity. By increasing ϵ', we push the whispering-gallery modes further into the resonator (11) Fig.4. This might greatly reduce the losses caused by surface defects such as dust or scratches. The change of the mode geometry also changes cavity radiative losses [29]. However, because radiative losses are usually insignificant compared with the losses due to surface scattering, we do not consider radiative losses here.

Moreover, an efficient coupling with whispering gallery modes may be achieved by a prism or fiber coupler that is in a physical contact with the dielectric cavity. This may significantly simplify usage of whispering gallery mode cavities outside a laboratory. Such a contact usually overloads the modes of a dielectric cavity and results in a significant broadening of the resonances. However, by engineering the profile of the dielectric susceptibility gradient we reduce the evanescent field of the cavity in such a way that the coupling is still possible but influence of the surface contamination is greatly suppressed.

Usually the quality factor of a WGM is determined by three effects: absorption in the material, Q_m, surface scattering losses, Q_{ss}, and loading by the external coupler, Q_l. The load quality factor can be regulated from outside. It depends on the distance, d, from the coupling prism to the sphere surface as follows

$$Q_l \sim \exp\left[\frac{4\pi d\sqrt{\epsilon_0 - 1}}{\lambda}\right], \quad (15)$$

where λ is the mode wavelength. The critical (optimum) coupling with the mode is achieved if d is chosen such that $Q_l = (1/Q_{ss} + 1/Q_m)^{-1}$. Because usually $Q_m \gg Q_{ss}$, one neglects by the absorption of the material.

Both Q_{ss} and Q_l are proportional to the ratio of the field power on the surface of the cavity and the total energy of the mode [33]. In other words, one can present the power of the losses because of the surface scattering and because of the coupler as $P_{ss} = \beta E(r=R)^2$ and $P_l = \alpha E(r=R)^2$, respectively, where α is a geometrical factor that depends on the shape and the dielectric constants of a coupler and a thin surface layer where WGM is localized, and on the distance between the coupler and the cavity surface; β depends on geometry of the surface inhomogeneities and their optical parameters, $E(r=R)$ is the amplitude of the electric field on the cavity surface.

The quality factor may be determined as $Q_{l,ss} = W/(P_{l,ss}T)$, where W is the energy stored in the mode, and T is the oscillation period. By changing the profile of the index of refraction $\epsilon(r)$ we change ratio $W/E(r=R)^2$ but Q_l/Q_{ss} stays unchanged. Therefore, choosing $Q_l/Q_{ss} = 1/2$ and reducing the absorption due to the surface scattering via engineering cavity index of refraction such that $Q_{ss} = Q_m$, we may reach both the critical coupling and the maximum index of refraction. Max-

imum achievable quality factors for silica microspheres are about $Q_m = 10^{12}$ [33].

For instance, to estimate the increase of the quality factors with the index gradient it is convenient to use a simple ratio. Let us consider two identical spherical microcavities except that the susceptibility of one cavity is constant ϵ_0 and the susceptibility of the other is space dependent $\epsilon(r)$ ($\epsilon(R) = \epsilon_0$). The ratio of the quality factors of the cavities is

$$\frac{Q_l}{\widetilde{Q}_l} \simeq \frac{Q_{ss}}{\widetilde{Q}_{ss}} \simeq \frac{\Psi^2(r=R)}{\int_0^R \Psi^2(r)dr} \frac{R(\epsilon_0 - 1)}{2\epsilon_0}. \qquad (16)$$

where Q_l and Q_{ss} ($\widetilde{Q}_l$ and $\widetilde{Q}_{ss}$) are the quality factors due to loading and surface scattering for the cavity with constant (graded) susceptibility, $\Psi(r) \sim E(r)$ is the field distribution of a TE mode of the graded cavity. The less is the field on the surface of the dielectric cavity $\Psi(r = R)$ (the deeper is the mode localization) the less is the absorption and coupling, and higher the quality factors. The dependence is shown in Fig.5.

Finally, let us consider a situation when a coupling prism is in a full contact with the dielectric cavity ($d = 0$). The coupling losses exceed the surface scattering losses in this case. We may increase Q_l changing $\epsilon(r)$ until the bulk optical losses become equal to the coupling losses. At this point we have critical coupling but at much higher Q-factor level.

It worth noting here, that in some cases it is important to increase evanescent field of a dielectric cavity, not to decrease it, as we discussed above. For example, if the cavity is intended to be used as an optical sensor. This problem also may be managed via a manipulation of $\epsilon(r)$ dependence. It has been shown that whispering gallery modes tend to be closer to the cavity surface if the index of refraction of the cavity close to its surface exceeds the internal index of refraction [29]. Such dependence of the refractive index will increase the surface absorption, but also it will increase the coupling to the external space.

D. Numerical simulations

Our approximation $1 \gg r'/R$ breaks down for $\epsilon' \to 2\epsilon_0/R$, so we are unable to infer the extend of the dispersion compensation and reshaping of the mode from this analytical calculations. Our exact numerical simulations show that the approximate analytical solution gives rather satisfactory results for the gradients less than the critical value.

Let us now solve the exact equation (4) with boundary conditions $\Psi(r = 0) = 0$ and $\Psi(r \to \infty) = 0$ numerically. The result is presented in Fig.1 and Fig.2. The second order dispersion vs gradient of the refractive index is shown in Fig.1. This dispersion determines the number of equidistant modes N (7). It is easy to see a good correspondence between the eigenvalues of the exact equation (4) (solid lines) and the first order approximation of this equation (10) (dashed lines). It is important to note that in the region $\epsilon' \geq 2\epsilon_0/R$, where Eq.10 is not valid, the second order dispersion becomes negative. This allows for compensation of the dispersion of the cavity host material which is not taken into account in our calculations. Except for the complete compensation point in the vicinity of $\epsilon' = 2\epsilon_0/R$, the dispersion decreases and reaches minimum of a half percent of the initial value for large gradients.

E. Suggestions for the implementation

It is not necessary to produce a cavity that has a gradient of the index of refraction in the entire cavity. The modes of the cavity are localized in the vicinity of the cavity surface (Fig.4). Therefore, the gradient may be localized in the vicinity of the surface as well.

For example, if we build a spherical cavity of 500 μm in radius from an optically homogeneous material and study modes with $\nu = 10^3$ and quality factor $Q = 10^8$, the mode spectrum is completely not equidistant. In turn, if the same cavity is fabricated from a graded material with $\epsilon'/\epsilon \approx 40$ cm^{-1} gradient of index in the vicinity of the cavity boundary $\Delta R \approx 5$ μm, at least a hundred modes of the cavity can be treated as equidistant.

For example, there are multimode fibers with germanium doped core ($\sqrt{\epsilon_0} \approx 1.5$) and pure silica clad ($\sqrt{\epsilon_0} \approx 1.45$). Originally the fiber has step-like dependence of the refractive index on the radius. Heating of the fiber results in diffusion of the Ge ions into the clad. This results in formation of the gradient in the refractive index.

Let us consider, for example, a fiber with 1 mm core diameter and 8 μm clad. In this case the gradient is closed to the critical one after thermal diffusion is realized.

On the other hand we may create a sphere from a high index flint glass ($\sqrt{\epsilon_0} \approx 1.7$) and cover it with fluoride glass ($\sqrt{\epsilon_0} \approx 1.4$). Subsequent thermalization will allow us to create gradients that even exceed critical one in thick surface layer.

IV. CONCLUSION

In conclusion, we have demonstrated that a number of important advantages can be achieved with a whispering-gallery mode microcavity fabricated from a material with graded index of refraction. Graded index material is widely available in the form of lenses and fibers. Such material can be formed into microcavities with standard mechanical and thermal fusion techniques. Main advantage of graded-index microcavity is that the spectrum of resonant frequencies is equidistant to first order. Secondly, the mode field is pushed away in a controlled way from the boundary to inside the dielectric, thereby deiminsihing the detrimental effect of surface roughness and

contamination. Finally, appropriately engineered near-surface gradient will eliminate the need for adjustable (and unstable) air gap between the WGM microcavity and evanescent coupler. This approach will be a major enhancement for a variety of applications, and a significant breaktrhrough enabling simple packaging solutions for practical devices. We expect that ultra-high-Q microcavities based on gradient-index approach, will not only enhance the performance and expand the range of applications, but provide a critical step towards their wide acceptance as a novel building block of modern photonics.

V. ACKNOWLEDGMENTS

The research described in this paper was carried out by the Jet Propulsion Laboratory, California Institute of Technology, under a contract with the National Aeronautics and Space Administration. AAS also acknowledges support from National Research Council.

[1] V. B. Braginsky, M. L. Gorodetsky, and V. S. Ilchenko, "Quality-factor and nonlinear properties of optical whispering gallery modes", Phys. Lett. A **137**, 393-397 (1989).

[2] L. Collot, V. Lefevre-Seguin, M. Brune, J.-M. Raimond, and S. Haroshe, "Very high-Q whispering-gallery mode resonances observed in fused silica microspheres", Europhys. Lett. **23**, 327-334 (1993).

[3] M. L. Gorodetsky, A. A. Savchenkov, and V. S. Ilchenko, "Ultimate Q of optical microsphere resonators", Opt. Lett. **21**, 453-455 (1996).

[4] D. W. Vernooy, V. S. Ilchenko, H. Mabuchi, E. W. Streed, and H. J. Kimble, "High-Q measurements of fused-silica microspheres in the near infrared", Opt. Lett. **23**, 247-249 (1998).

[5] H. M. Tzeng, K. F. Wall, M. B. Long, and R. K. Chang, "Laser emission from individual droplets at wavelengths corresponding to morphology-dependent resonances", Opt. Lett. **9**, 499-501 (1984).

[6] J. C. Knight, H. S. T. Driver, R. J. Hutcheon, and G. N. Robertson, "Core resonance capillary fiber whispering gallery mode laser", Opt. Lett. **17**, 1280-1282 (1992).

[7] A. F. J. Levi, S. L. McCall, S. J. Pearton, and R. A. Logan, "Room-temperature operation of submicrometer radius disk laser", Electron. Lett. **29**, 1666-1668 (1993).

[8] V. Sandoghdar, F. Treussart, J. Hare, V. Lefevre-Seguin, J. M. Raimond, and S. Haroche, "Very low threshold whispering-gallery-mode microsphere laser", Phys. Rev. A **54**, R1777-R1780 (1996).

[9] F. Treussart, V. S. Ilchenko, J. F. Roch, P. Domokos, J. Hare, V. Lefevre, J. M. Raimond, and S. Haroche, "Whispering gallery mode microlaser at liquid Helium temperature", J. Lumin. **76**, 670-673 (1998).

[10] F. Treussart, V. S. Ilchenko, J. F. Roch, J. Hare, V. Lefevre-Seguin, J. M. Raimond, and S. Haroche, "Evidence for intrinsic Kerr bistability of high-Q microsphere resonators in superfluid helium", Eur. Phys. J. D **1**, 235-238 (1998).

[11] M. Pelton and Y. Yamamoto, "Ultralow threshold laser using a single quantum dot and a microsphere cavity", Phys. Rev. A **59**, 2418-2421 (1999).

[12] A. N. Oraevsky, M. O. Scully, T. V. Sarkisyan, and D. K. Bandy, "Using whispering gallery modes in semiconductor microdevices", Laser Physics **9** , 990-1003 (1999).

[13] M. Cai, O. Painter, K. J. Vahala, and P. C. Sercel, "Fiber-coupled microsphere laser", Opt. Lett. **25**, 1430-1432 (2000).

[14] F. Lissillour, P. Feron, N. Dubreuil, P. Dupriez, M. Poulain, and G. M. Stephan, "Erbium-doped microspherical lasers at 1.56 μm", Electron. Lett. **36**, 1382-1384 (2000).

[15] Y. S. Choi, H. J. Moon, K. Y. An, S. B. Lee, J. H. Lee, and J. S. Chang, "Ultrahigh-Q microsphere dye laser based on evanescent-wave coupling", J. Korean Phys. Soc. **39**, 928-931 (2001).

[16] D. W. Vernooy, A. Furusawa, N. P. Georgiades, V. S. Ilchenko, and H. J. Kimble, "Cavity QED with high-Q whispering gallery modes", Phys. Rev. A **57**, R2293-R2296 (1998).

[17] G. Annino, M. Cassettari, M. Fittipaldi, L. Lenci, I. Longo, M. Martinelli, C. A. Massa, and L. A. Pardi, "Whispering gallery mode dielectric resonators in EMR spectroscopy above 150 GHz: Problems and perspectives", Appl. Magn. Reson. **19**, 495-506 (2000).

[18] V. S. Ilchenko, X. S. Yao, and L. Maleki, "Microsphere integration in active and passive photonics devices", Proc. SPIE **3930**, 154-162 (2000).

[19] V. S. Ilchenko and L. Maleki, "Novel whispering-gallery resonators for lasers, modulators, and sensors", Proc. SPIE **4270**, 120-130 (2001).

[20] W. von Klitzing, R. Long, V. S. Ilchenko, J. Hare, and V. Lefevre-Seguin, "Tunable whispering gallery modes for spectroscopy and CQED experiments", New J. Phys. **3**, 141-144 (2001).

[21] S. Blair and Y. Chen, "Resonant-enhanced evanescent-wave fluorescence biosensing with cylindrical optical cavities", Appl. Optics **40**, 570-582 (2001).

[22] R. W. Boyd and J. E. Heebner, "Sensitive disk resonator photonic biosensor", Appl. Optics **40**, 5742-5747 (2001).

[23] A. Eschmann and C. W. Gardiner, "Stability and switching in whispering gallery mode microdisk lasers", Phys. Rev. A **49**, 2907-2913 (1994).

[24] F. C. Blom, D. R. van Dijk, H. J. W. M. Hoekstra, A. Driessen, and T. J. A. Pompa, "Experimental study of integrated-optics microcavity resonators: Toward an all-optical switching device", Appl. Phys. Lett. **71**, 747-749 (1997).

[25] J. Popp, M. H. Fields, and R. K. Chang, "Q switching by saturable absorption in microdroplets: elastic scattering and laser emission", Opt. Lett. **22**, 1296-1298 (1997).

[26] J. E. Heebner and R. W. Boyd, "Enhanced all-optical switching by use of a nonlinear fiber ring resonator", Opt. Lett. **24**, 847-849 (1999).

[27] V. V. Klimov, M. Ducloy, and V. S. Letokhov, "Strong

interaction between a two-level atom and the whispering-gallery modes of a dielectric microsphere: Quantum-mechanical consideration", Phys. Rev. A **59**, 2996-3014 (1999).

[28] V. S. Ilchenko, M. L. Gorodetsky, X. S. Yao, and L. Maleki, "Microtorus: a high-finesse microcavity with whispering-gallery modes", Opt. Lett. **26**, 256-258 (2001).

[29] D. Q. Chowdhury, S. C. Hill, and P. W. Barber, "Morphology-dependent resonances in radially inhomogeneous spheres", J. Opt. Soc. Am. A **8**, 1702-1705 (1991).

[30] Equation for TM modes looks similar, however we do not consider it here for the sake of clarity.

[31] C. C. Lam, P. T. Leung, and K. Young, "Explicit asymptotic formulas for the positions, widths, and strengths of resonances in Mie scattering", J. Opt. Soc. Am. B **9**, 1585-1592 (1992).

[32] L. G. Guimaraes and H. M. Nussenzveig, "Theory of Mie resonances and ripple fluctuations", Opt. Comm. **89**, 363-369 (1992).

[33] M. L. Gorodetsky, A. D. Pryamikov, and V. S. Ilchenko, "Rayleigh scattering in high-Q microspheres", J. Opt. Soc. Am. B **17**, 1051-1057 (2000).

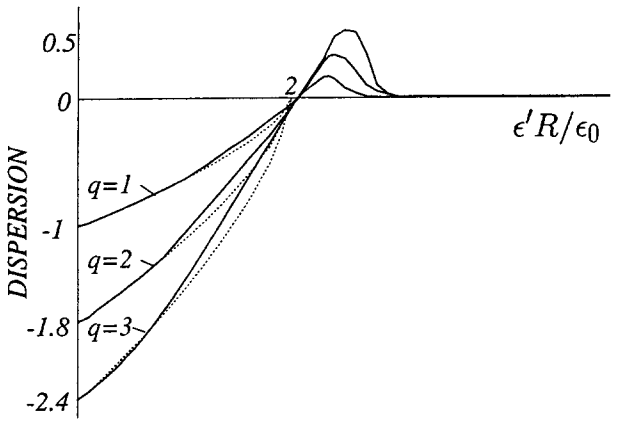

FIG. 1: Normalized second order dispersion $\partial^2 k_{q,\nu}/(\partial k_{q,\nu}^2)$ vs normalized gradient of the index of refraction of the material $\epsilon' R/\epsilon_0$ for $\nu_0 \approx 600$. Unity dispersion corresponds to $|\partial^2 k_{1,\nu}/(\partial k_{1,\nu}^2)|_{\epsilon'=0}$ at $\nu = \nu_0$.

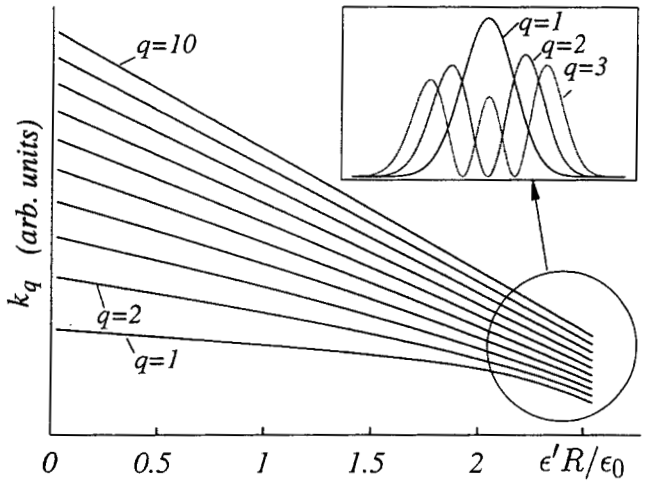

FIG. 2: Dependence of wave vector eigenvalues $k_{q,\nu}$ on normalized gradient of the index of refraction $\epsilon' R/\epsilon_0$ for $\nu \approx 600$. Modes with different q become closer with gradient increase. The modes pushed far away from the cavity boundary are nearly equidistant. Inset: Amplitude profile for the fields for large index gradients. The mode wave-functions are nearly symmetric.

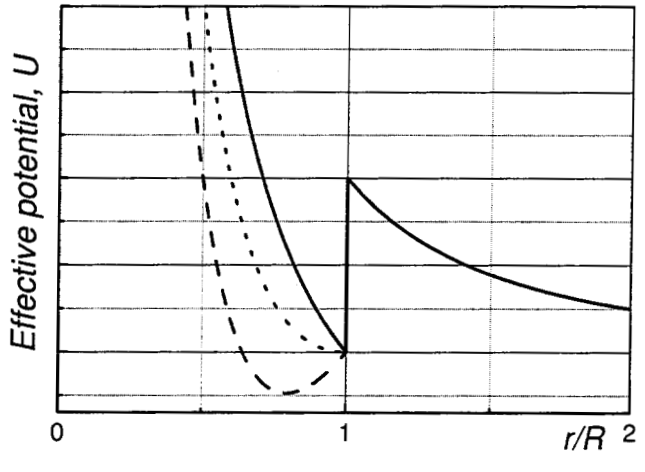

FIG. 3: Effective optical potential U for a transparent dielectric resonator with radius R. Solid line stands for $\epsilon(r)$ =const $(R > r)$; short dash – for $\epsilon(r) = \epsilon_0(3 - 2r/R)$ (critical gradient), long dash – for $\epsilon(r) = \epsilon_0(5 - 4r/R)$.

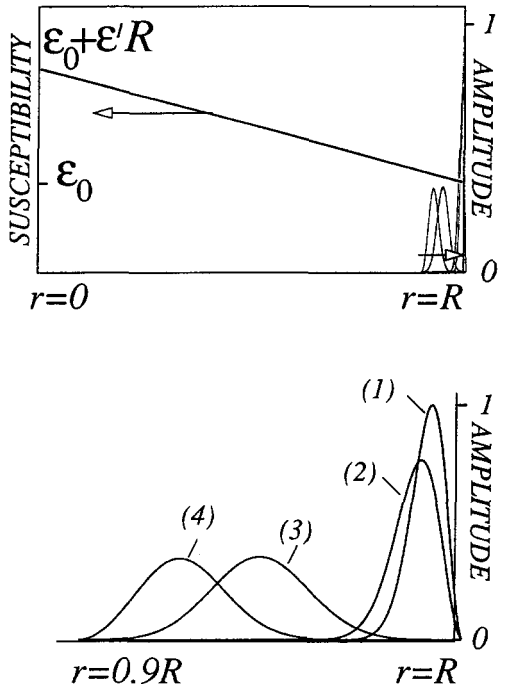

FIG. 4: Radial dependencies of the susceptibility of a cavity material as well as of the amplitude profiles of the field ($q = 1$) inside the cavity for various ϵ'. Top plot shows real scale for the filed distributions in case $\nu_0 = 600$. The fields are localized close to the cavity surface. The bottom plot shows the amplitude profiles in detail. Curve (1) of the bottom plot corresponds to $\epsilon' R/\epsilon_0 = 0$, (2) $\epsilon' R/\epsilon_0 = 1$, (3) $\epsilon' R/\epsilon_0 = 2$, and (4) $\epsilon' R/\epsilon_0 = 2.4$. It is easy to observe pushing of the mode out of the cavity boundary ($r = R$) and into the cavity.

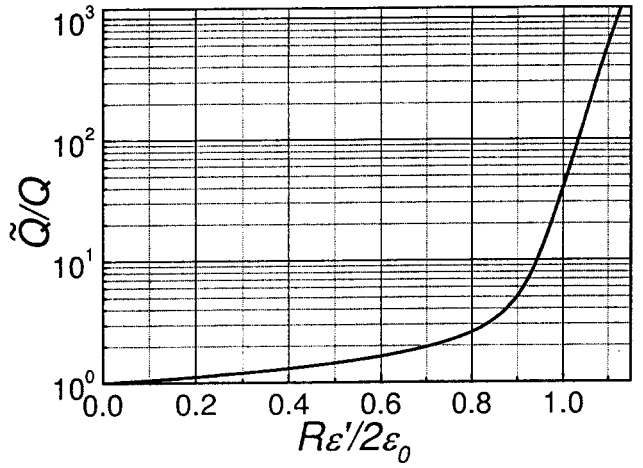

FIG. 5: Quality factor $\widetilde{Q}$ of a cavity with a gradient of the refractive index normalized by the quality factor Q of a cavity of the same radius without the gradient vs normalized gradient of the refractive index. The plot is created for a cavity with radius $R = 4$ mm, susceptibility $\epsilon_0 = 2.1$, and the mode wavelength $\lambda = 1.55$ μm.